Realization of X-Band Waveguide Filters by Low-Cost FDM Additive Manufacturing Techniques

Daniel Miek[1], Kennet Braasch[2], Sebastian Simmich[3], Fynn Kamrath[4], Patrick Boe[5], Michael Höft[6]

Chair of Microwave Engineering, Kiel University, Kaiserstr. 2, 24143 Kiel, Germany

{[1]dami, [2]stu122501, [3]ssi, [4]flk, [5]pabo, [6]mh}@tf.uni-kiel.de

***Abstract* — In this paper the realization of X-band waveguide filters in low-cost additive manufacturing (AM) techniques is discussed. All filters proposed here are manufactured with the economic fused deposition modeling (FDM) technique, which is very robust and has the smallest acquisition cost/overheads in comparison to other 3-D printing techniques commercially available. Six third-order filters are compared within this paper in terms of manufacturing accuracy, available Q-factor and spurious mode performance. The filter designs are discussed as well as the realization in the low-cost FDM printing technique. The galvanization as the last step of the realization process is addressed within this paper as well. The measurements show good agreement with the simulation.**

***Keywords* — 3-D printing, additive manufacturing (AM), fused deposition modeling (FDM), waveguide filter, X-band.**

I. Introduction

Additive manufacturing techniques have become an easy and fast opportunity for the realization of functional components [1], [2]. In the beginning these techniques were mainly limited to the realization of non-functional components. However, today the accuracy of most AM techniques is high enough that even functional parts can be manufactured very fast and without much effort. Furthermore, AM offers possibilities for the design and realization of filter structures, which are not possible to implement with classical manufacturing techniques, e.g. milling.

Different additive manufacturing techniques are available on the market. They can be classified in e.g. the material which is processed, the acquisition cost, the overheads as well as the desired manufacturing accuracy [1], [2]. Often the application of the parts to be manufactured decides about the printing technique. From the material point of view the selective laser melting (SLM) should be preferred for the realization of waveguide filters, as the workpiece can be directly manufactured from a metallic material. However, the cost of the printing system as well as the additional overhead is very high.

On the one hand, the FDM technique is a low-cost but sufficient alternative. In the workflow a plastic material (filament) is heated by a nozzle and extruded on a platform at positions defined by the slicer, which processes the CAD file. The acquisition cost of an ordinary printer lies below 600 Euro while the overheads only comprise the filament for the object to be printed. The manufacturing accuracy is controlled by settings as for example the layer height and the printing speed. On the other hand, stereolithography (SL) based printing techniques were often used in the manufacturing of waveguide components [3], [4]. However, compared to the FDM technique, the acquisition cost as well as the overheads are higher. The parts are manufactured from a liquid resin which is cured by an UV-light at positions defined by the CAD file. The resin must periodically be renewed and the printing accuracy strongly depends on the cleanliness of the optical system which aligns the UV-laser. In this paper it is shown that the accuracy of the FDM manufacturing technique is sufficient for the realization of at least X-band waveguide filters, which can lower the overall manufacturing cost drastically.

This paper is organized as follows: In Sec. II the design and realization of single-mode waveguide filters is discussed. Six third-order filters are manufactured, measured and compared with each other in terms of printing accuracy, maximal available Q-factor, spurious mode performance and the filter volume. In Sec. III the measurement results are discussed while Sec. IV gives a short overview over the manufacturing/galvanization process. Sec. V concludes this paper.

II. Realization of third order filters

Six waveguide filters are investigated and compared within this paper. The specifications among the filters are identical to allow an easy comparability. All filters are of third order and designed to achieve a return loss of $RL \approx 25\,\mathrm{dB}$. The lower and upper band edges are set to $f_1 = 10\,\mathrm{GHz}$ and $f_2 = 10.5\,\mathrm{GHz}$, respectively ($f_0 = 10.25\,\mathrm{GHz}$, $B = 500\,\mathrm{MHz}$, $FBW = 4.88\,\%$). No transmission zeros are foreseen to keep the design simple, leading to the following coupling matrix coefficients [5]: $m_{S1} = m_{3L} = 1.2214$, $m_{12} = m_{23} = 1.2197$. The proposed third order filters are shown in Fig. 1 (a)-(f). The filters mainly differ in the realization of the resonators as well as the coupling apertures. However, the main steps of the design process are identical. Initially, all resonators are designed to operate at their basic mode, which is done by an eigenmode-analysis. Subsequently, the dimensions of the coupling apertures can be determined by considering the first two eigenmodes of two coupled resonators. By evaluating (1) the relationship between the internal coupling matrix coefficients and the dimension of the coupling aperture is found in terms of the eigenmodes f_1 and f_2 [6].

$$m_{ij} = \frac{f_2^2 - f_1^2}{f_2^2 + f_1^2} \cdot \frac{1}{FBW} \tag{1}$$

ISBN 978-3-9820397-1-8

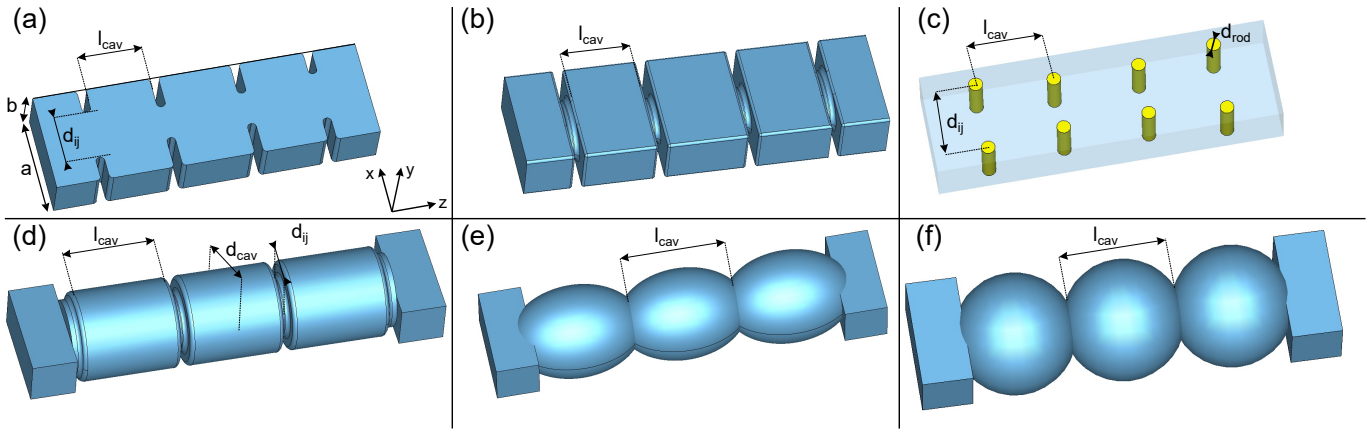

Fig. 1. Schematic drawing of the realized filters: (a)-(c) Rectangular cavities with rectangular, elliptical and post coupling apertures, respectively, (d) circular cavities with circular blends, (e) elliptical cavities and (f) spherical cavities. All filters (except (c)) are printed in two halves, while the y-z plane defines the cutting plane which coincide with the E-plane of the filters.

The dimensions of the input/output coupling iris can be calculated based on e.g. the evaluation of the group delay [6]. Furthermore, it is also possible to "convert" the external couplings m_{S1} and m_{3L} into internal ones as proposed in [7]. The calculation of the coupling aperture dimension is then basically accomplished based on (1). The tuning of the resonator length l_{cav} can subsequently be done by coupling matrix extraction and tuning techniques [8], [9].

A. *Filter structures*

Six third-order filter set-ups are manufactured with the low-cost additive manufacturing FDM technique. Schematic illustrations are shown in Fig. 1 (a)-(f). The input and output waveguides are designed to realize the X-band waveguide standard ($a = 22.86\,\text{mm}$, $b = 10.16\,\text{mm}$).

(a) In Fig. 1 (a) the most basic type of an inductive coupled waveguide filter is shown. The width and height of the resonators correspond to the X-band standard. The length of the resonators (l_{cav}) as well as the blend width (d_{ij}) can be found as described above. The resonators are designed to operate at their basic TE_{101}-mode. All edges have radii to ease the copper-plating procedure. For the manufacturing process the filter is cut in two halves along the y-z plane (which corresponds to the electrical E-plane) to reduce losses. No surface currents are disturbed by using this cutting plane.

(b) A further third order filter based on rectangular resonators but coupled with elliptic irises is shown in Fig. 1 (b). The coupling strength can be adapted by varying mainly the width of the elliptic blends. In the manufacturing process this filter is cut in the E-plane (y-z plane) as well.

(c) Fig. 1 (c) shows the last filter which is based on rectangular resonators. The blends are realized by inductive posts as basically proposed in [10]. All posts have the same diameter of $d_{rod} = 3\,\text{mm}$ while the coupling strength can be adapted by the position of the posts along the x-axis. The closer the posts are positioned to the side wall of the cavity, the larger is the achievable coupling factor. Fig. 2 shows the coupling strength as calculated by (1) if the division by the fractional bandwidth is omitted. If the distance between the posts or the diameter of the posts is enlarged, the coupling factor can be increased. The filter housing is printed and spray-coated in one piece while the posts are manufactured separately. To avoid support material inside the waveguide channel, the filter is printed in z-direction. Subsequently, the galvanization takes places after the posts are inserted into the filter.

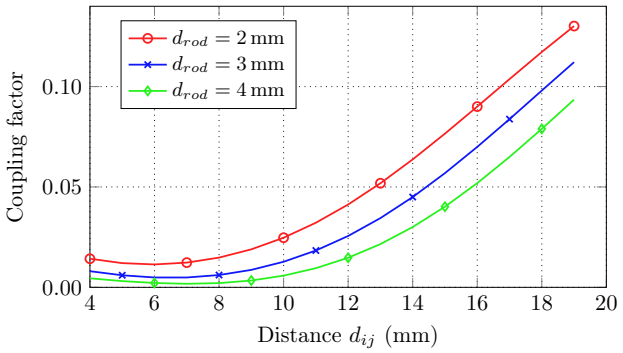

Fig. 2. Coupling factor of the post coupling aperture in dependency of the distance between the posts d_{ij} with post diameter as parameter.

(d) In Fig. 1 (d) a filter based on cylindrical resonators is shown. The resonators have a length of $l_{cav} \approx 22\,\text{mm}$ and diameter $d_{cav} = 20\,\text{mm}$. The resonant mode used here is the fundamental TE_{111}-mode. The length of the resonators is used to tune the center frequency. The couplings in between the cavities are designed as circular apertures, which coupling factor might be adapted by changing the diameter. Please note that the TE_{111}-mode can also be used in dual-mode operation due to the rotational symmetry of the mode. In this case distortions must be inserted in the cavity to tune both modes for parallel excitation [11]. In the simulation the orthogonal dual-modes are not excited as no distortions are foreseen.

ISBN 978-3-9820397-1-8

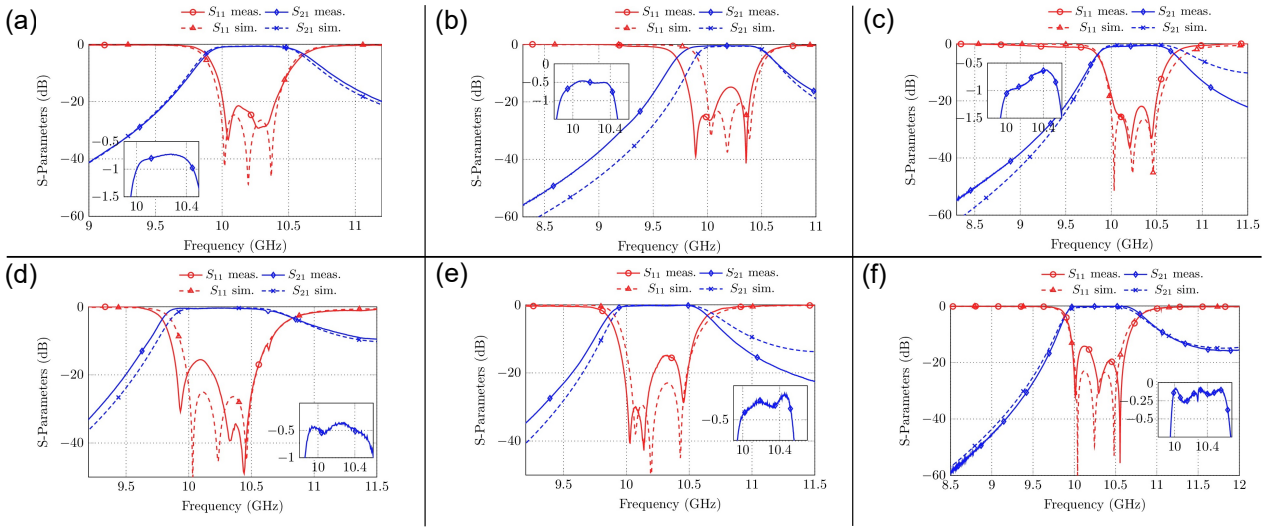

Fig. 3. Overview of the S-parameter responses for the filter structures shown in Fig. 1. The results are obtained without tuning screws, as they are not foreseen in the proposed filters.

However, due to manufacturing uncertainties or irregular galvanization the dual-modes might be excited, leading to distortions in the passband of the filter.

(e) A similar approach is shown in Fig. 1 (e). Here, elliptic formed cavities are used to implement three resonances. As in (d), dual-mode operation could be achieved by the insertion of distortions within the cavities. However, the orthogonal mode induces currents which flow in the cutting plane, leading to increased insertion losses. The couplings are realized by the apertures which are formed when two adjacent cavities are superimposed. The length of the superposition determines the coupling strength. This set-up provides many advantages with additive manufacturing techniques due to the smooth transitions between the cavities which is also beneficial in the galvanization process.

(f) The last set-up proposed here is based on spherical resonators as shown in Fig. 1 (f). The couplings are again realized by the superposition of the adjacent cavities while the resonance frequencies might by adapted by the diameter of the resonators l_{cav}.

B. Comparison

1) Spurious mode performance

An important requirement for filters with strong attenuation specifications in the stopband is the spurious mode performance. Rectangular shaped resonators show usually a good spurious mode performance among the waveguide filters. The set-ups in Fig. 1 (a)-(c) operate in their basic TE_{101}-mode. The next resonance is the TE_{102}-mode which occurs at approximately 15.5 GHz and is above the usable frequency region of the TE_{10} fundamental waveguide mode.

The set-up shown in Fig. 1 (d) is based on cylindrical resonators and exploits the TE_{111} fundamental mode. Due to the rotational symmetry, two modes at the same frequency might be excited and allow dual-mode operation. However, if distortions in the symmetry are avoided the orthogonal mode is not excited as desired here. The first spurious mode is excited at approximately 12.5 GHz. Similar statements can be made for the elliptic and spherical resonators, where the first spurious modes arise at 12.5 GHz and 13 GHz, respectively. The results are summarized in Tab. 1.

2) Quality factor and volume

An important measure to characterize the losses which arise in the filter is the Q-factor. Generally speaking, larger resonator volumes lead to higher available quality factors. The Q-factor of the simulation (assuming a 50 % conductivity of ideal copper) is compared with the Q-factor of the measurement in Tab. 1 for all filter geometries. From the simulation point of view, the highest available Q-factor can be expected from the spherical resonators while the rectangular based waveguide filters show the lowest value, however, this is in contrast to the required volume and the spurious-mode performance. The volumes in Tab. 1 are calculated by considering only the vacuum which realizes the resonator geometry as well as a feed-line of 10 mm length. The measured Q-factor strongly depends on the success of the galvanization process. On the one hand the galvanized surface should have a thickness of several skin-depths while on the other hand the dimensions of the filter should not be modified too much. Therefore, smooth structures which allow an uniform deposition of copper are preferred. For this reason, curvy structures like the spherical resonator based filter may reach a quality factor of $Q_u \approx 2400$, while the Q-factors of the rectangular based filters are much lower. The galvanization of the faces near to the blend as well as the blend itself is problematic and assumed to be the reason for the low Q-factor. The surface roughness may also slightly decrease the Q-factor of all measurements and was determined from a test sample (after spray coating and galvanization) to be $S_a \approx 3\,\mu$m, where S_a describes the mean arithmetic height of the surface.

ISBN 978-3-9820397-1-8

Table 1. Comparison of the proposed filters in terms of Q-factor, measured insertion loss [dB], spurious mode performance [GHz], volume [cm^3] and the manufacturing cut.

	(a)	(b)	(c)	(d)	(e)	(f)
Q_u sim.	4683	4679	4525	6873	7484	7625
Q_u meas.	390	450	310	490	700	2400
IL meas.	0.7	0.5	0.9	0.45	0.4	0.2
Spur.	15.5	15.5	15.5	12.5	12.5	13
Volume	16.1	16.2	17.3	26.5	25.8	26.3
Cut	E-pl.	E-pl.	no cut	E-pl.	E-pl.	E-pl.

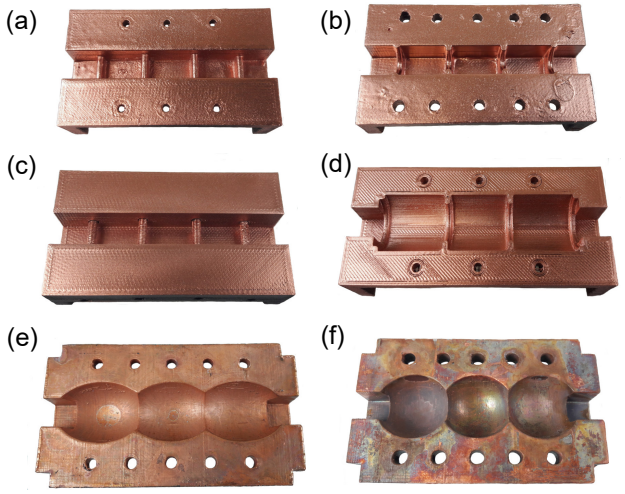

Fig. 4. Overview over manufactured filter halves: (a) rectangular waveguide filter, (b) rectangular waveguide filter with elliptic blends, (c) rectangular waveguide filter with post coupling, (d) cylindrical resonator filter, (e) elliptical resonator filter and (f) spherical resonator filter. All halves are spray coated (half (f) is also galvanized).

III. Measurement Results

The measurement results in comparison to the simulation are summarized in Fig. 3 (a)-(f) corresponding to the filter set-ups in Fig. 1 (a)-(f). In most cases the measured return loss as well as the band edges coincide with the desired parameters. Some S-parameters show a small frequency shift which is caused by manufacturing inaccuracies. Nevertheless, the accuracy of the printing system is high enough for the manufacturing of the proposed filter set-ups.

Fig. 4 shows manufactured halves of all proposed filters. Please note that the post-based filter is manufactured in one piece and the half in Fig. 4 (c) is only shown for clarification.

IV. Manufacturing Techniques

All filters proposed here are manufactured with the economic FDM printing technique. A nozzle diameter of $d_n = 0.4\,\text{mm}$ is used while smaller diameters (e.g. 0.2 mm) are commercially available as well. To achieve a good printing accuracy the maximal layer height is set to $h_l = 0.1\,\text{mm}$. The filters are manufactured with PLA material as a compromise between costs and processibility. As common in the FDM printing technique, no bulky parts are manufactured as in the inside a honeycomb structure is foreseen. The infill percentage is set to 40 % as a trade-off between robustness of the part and manufacturing time. The printing direction strongly effects the dimensional accuracy. Therefore, the filters are positioned on the building platform in a way that support-structures within the cavities are avoided (which corresponds to the y-axis in Fig. 1 except for the post-based filter, which is printed in z-direction). The post-filter is printed in one piece and the posts are inserted separately after spray coating but before the galvanization. After printing the filters are degreased and spray-coated with a commercially available copper spray. This step is necessary as PLA is not conductive. Nevertheless, the conductivity of the spray is far below the conductivity of pure copper which makes a subsequent galvanization necessary, which is accomplished in a bath based on sulfuric acid.

V. Conclusion

In this paper six third-order X-band waveguide filters are compared with each other in terms of manufacturing accuracy, available and measured Q-factor, spurious mode performance and filter volume. All filters are manufactured using the low-cost FDM printing technique followed by a subsequent galvanization. The comparison between simulation and measurement shows, that the printing accuracy of FDM manufacturing is sufficient for the realization of at least X-band waveguide filters. The measured insertion loss and hence the quality factor depends on the success of the galvanization process. As a result, the manufacturing accuracy is similar in all investigated cases. Nevertheless, the galvanization process gives better results if edges or shadowing are avoided.

References

[1] F. Calignano *et al.*, "Overview on additive manufacturing technologies," *Proc. IEEE*, vol. 105, no. 4, pp. 593–612, Apr. 2017.

[2] R. Sorrentino and O. A. Peverini, "Additive manufacturing: a key enabling technology for next-generation microwave and millimeter-wave systems," *Proc. IEEE*, vol. 104, no. 7, pp. 1362–1366, Jul. 2016.

[3] M. Dionigi, C. Tomassoni, G. Venanzoni, and R. Sorrentino, "Simple high-performance metal-plating procedure for stereolithographically 3-D-printed waveguide components," *IEEE Microwave and Wireless Components Letters*, vol. 27, no. 11, pp. 953–955, Nov. 2017.

[4] C. Guo, X. Shang, J. Li, F. Zhang, M. J. Lancaster, and J. Xu, "A lightweight 3-D printed X-band bandpass filter based on spherical dual-mode resonators," *IEEE Microwave and Wireless Components Letters*, vol. 26, no. 8, pp. 568–570, Aug. 2016.

[5] R. J. Cameron, C. M. Kudsia, and R. R. Mansour, *Microwave Filters for Communication Systems*. Wiley, 2007.

[6] J.-S. Hong and M. J. Lancaster, *Microstrip Filters for RF/Microwave applications*. John Wiley & Sons Inc., 2001.

[7] X. Shang, W. Xia, and M. J. Lancaster, "The design of waveguide filters based on cross-coupled resonators," *Microwave and Optical Technology Letters*, vol. 56, no. 1, pp. 3–8, Nov. 2013.

[8] G. Macchiarella and D. Traina, "A formulation of the cauchy method suitable for the synthesis of lossless circuit model of microwave filter from lossy measurements," *IEEE Microwave and Wireless Components Letters*, vol. 16, no. 5, pp. 243 – 245, May 2006.

[9] G. Macchiarella, "Extraction of unloaded Q and coupling matrix from measurements on filters with large losses," *IEEE Microwave and Wireless Components Letters*, vol. 20, no. 6, pp. 307–309, Jun. 2010.

[10] I. Hunter, *Theory and Design of Microwave Filters*. IET, 2001.

[11] S. Amari and M. Bekheit, "Physical interpretation and implifications of similarity transformations in coupled resonator filter design," *IEEE Trans. MTT.*, vol. 55, no. 6, pp. 1139–1153, Jun. 2007.

ISBN 978-3-9820397-1-8